



Stochastic adaptive control model for traffic signal systems

X.-H. Yu ^{a,1}, W.W. Recker ^{b,*}

^a Department of Electrical Engineering, California Polytechnic State University, San Luis Obispo, CA 93407, USA

^b Department of Civil and Environmental Engineering, Institute of Transportation Studies, University of California, Irvine, CA 92697, USA

Abstract

An adaptive control model of a network of signalized intersections is proposed based on a discrete-time, stationary, Markov decision process. The model incorporates probabilistic forecasts of individual vehicle actuations at downstream inductance loop detectors that are derived from a macroscopic link transfer function. The model is tested both on a typical isolated traffic intersection and a simple network comprised of five four-legged signalized intersections, and compared to full-actuated control. Analyses of simulation results using this approach show significant improvement over traditional full-actuated control, especially for the case of high volume, but not saturated, traffic demand.

© 2006 Published by Elsevier Ltd.

Keywords: Adaptive control; Traffic signal systems; Markov processes; Traffic

1. Introduction

At a signalized intersection, traffic signals typically operate in one of three different control modes: pre-timed control, semi-actuated control and full-actuated control (Wilshire et al., 1985). In pre-timed control, all of the control parameters are fixed and preset off-line. Off-line techniques (e.g., the various versions of the TRANSYT (Robertson, 1969) family of software packages) are useful in generating the parameters for fixed timing plans for conventional pre-timed urban traffic control systems based on the deterministic traffic conditions during different time periods of the day (e.g., peak hours, off-peak hours). In actuated (both semi- and full-)control, the control signal is adjusted in accordance with a “closed-loop, on-line” control strategy based on real-time traffic demand measures obtained from detectors; while the controllers themselves respond to the fluctuations of the traffic flows in the network, the base parameters do not. Alternatively, a class of control algorithms that includes SCOOT (Split, Cycle And Offset Optimization Technique) (Hunt et al., 1982; Robertson and Bretherton, 1991) and SCATS (Sydney Coordinated Adaptive Traffic System) (Lowrie, 1982) are generally considered to be “on-line” algorithms, in which the control strategy is to “match” the current traffic conditions obtained from detectors to the “best” pre-calculated off-line timing plan.

* Corresponding author. Tel.: +1 949 824 5642/5989; fax: +1 949 824 8385.

E-mail addresses: xhyu@calpoly.edu (X.-H. Yu), wwrecker@uci.edu (W.W. Recker).

¹ Tel.: +1 805 756 2441.

31 Far fewer well-tested examples exist of real-time adaptive traffic control systems that react to actual traffic
 32 conditions on-line, the most notable among these being the well-known OPAC algorithm (Gartner, 1983), and
 33 RHODES™, a real-time traffic-adaptive signal control system that uses a traffic flow arrivals algorithm (Head,
 34 1995) based on detector information to predict future traffic volume.

35 In general, two issues must be addressed to achieve real-time adaptive traffic control: (1) development of a
 36 mathematical model for the control of the stochastic, highly nonlinear traffic system, and (2) design of an
 37 appropriate control law such that the behavior of the system meets certain performance indices (e.g., mini-
 38 mum queue length, minimum delay time, etc.). Mathematical models used for the representation of traffic phe-
 39 nomena on signalized surface street networks can be classified into the following three generalized categories:
 40 (1) store-and-forward models (Hakimi, 1969; Singh and Tamura, 1974; D'Ans and Gazis, 1976), (2) disper-
 41 sion-and-store models (Cremer and Schoof, 1989; Chang et al., 1994), and (3) kinematic wave models (Ste-
 42 phanedes and Chang, 1993; Lo, 2001).

43 There are two fundamental approaches for on-line optimization: binary choice logic and the sequential
 44 approach. In the binary choice logic approach, time is divided into successive small intervals, and a binary
 45 decision is made either to extend the current signal phase by one interval, or to terminate it. Examples of this
 46 approach include Miller's algorithm, traffic optimization logic (TOL), modernized optimized vehicle actua-
 47 tion strategy (OVA), stepwise adjustment of signal timing (SAST), etc. (Lin, 1989; Lin and Vijayakumar,
 48 1989). The drawback of this approach is that it only considers a very short future time interval (usually 3–
 49 6 s) for the decision, and thus cannot guarantee the overall optimization of the signal operation. In the
 50 sequential approach, the length of a decision-making stage is relatively longer (from 50 to 100 s) to more clo-
 51 sely approach the long-term optimal control. In OPAC, developed explicitly for real-time traffic control, the
 52 alternative disadvantages of the binary and sequential approaches are mitigated by incorporating a rolling-
 53 horizon approach; however, its application formally is limited to isolated intersections. Artificial neural net-
 54 works (ANN) also have been applied to finding the solution for traffic control problems (Nakatsuji and
 55 Kaku, 1991) through an assumed mapping between the control variables (e.g., the split) and the objective
 56 function (e.g., the queue length); the neural network is trained off-line, using the nonlinear mapping ability
 57 of ANN, to realize this relationship. Then the signal optimization is performed on-line, using the self-orga-
 58 nization property of an ANN. The training algorithm is a stepwise method (combination of a Cauchy
 59 machine and the "back-propagation" algorithm). However, this approach is valid only when the traffic sys-
 60 tem is in steady state.

61 Although most existing adaptive signal control strategies incorporate an implicit recognition that traffic
 62 conditions are time variant due to random processes, they generally adopt explicitly deterministic control
 63 models. Additionally, most employ heuristic control strategies without an embedded traffic flow model. Alter-
 64 natively, the random nature of the traffic system lends itself more directly to a stochastic control approach. In
 65 the work reported here, a stochastic traffic signal control scheme, based on Markovian decision control, is
 66 introduced. The objective is to develop a real-time adaptive control strategy that explicitly incorporates the
 67 random nature of the traffic system in the control. A Markov control model is first developed; then the signal
 68 control problem is formulated as a decision-making problem for the Markov model. This approach is tested
 69 both on a typical isolated traffic intersection and a simple network comprised of five four-legged signalized
 70 intersections, and compared to full-actuated control. Analyses of simulation results using this approach show
 71 significant improvement over traditional full-actuated control, especially for the case of high volume traffic
 72 demand.

73 2. Markov control model

74 A stochastic process $x(t)$ is called Markov (Papoulis, 1984) if its future probabilities are determined by its
 75 most recent values; i.e., if for every n and $t_1 < t_2 \cdots < t_n$

$$77 \quad P(x(t_n) \leq x_n | x(t) \forall t \leq t_{n-1}) = P(x(t_n) \leq x_n | x(t_{n-1})).$$

78 The adaptive control algorithm proposed is based on a discrete-time, stationary, Markov control model
 79 (also known as a Markov decision process or Markov dynamic programming) defined on $(\mathbf{X}, \mathbf{A}, \mathbf{P}, \mathbf{R})$, where

- 80 1. \mathbf{X} , a Borel² space, is the state space and every element in the space $x \in \mathbf{X}$ is called a state;
 81 2. \mathbf{A} , also a Borel space, is defined as the set of all possible controls (or alternatives). Each state $x \in \mathbf{X}$ is asso-
 82 ciated with a non-empty measurable subset $\mathbf{A}(x)$ of \mathbf{A} whose elements are the admissible alternatives when
 83 the system is in state x ;
 84 3. \mathbf{P} , a probability measure space in which an element p_{ij}^k denotes the transition probability from state i to
 85 state j under alternative action k ; and
 86 4. \mathbf{R} , a measurable function, also called a one-step reward.

87
 88 Selection of a particular alternative results in an immediate reward and a transition probability to the next
 89 state. The total expected discounted reward over an infinite period of time is defined as

$$91 \quad V \underline{\underline{A}} E \left[\sum_{t=0}^{\infty} \beta^t r(x_t, a_t) \right], \quad (1)$$

92 where $r(\cdot)$ is the one-step transition reward, β^t ($0 \leq \beta^t \leq 1$) is the discount factor, and a is the policy. The opti-
 93 mal reward v^* , or the supremum (least upper bound) of V , is defined as

$$95 \quad v^*(x, a^*) = \sup_{a \in \mathbf{A}} [V(x, a)]. \quad (2)$$

96 It can be obtained by solving a functional equation (also called the dynamic programming equation, or DPE):

$$98 \quad v^* = Tv^*, \quad (3)$$

99 where T is a contraction operator³ and

$$102 \quad Tv(x) = \max_{a \in \mathbf{A}} \left[q(x, a) + \beta \sum_{j=1}^N v(x) p_{ij}^a \right]. \quad (4)$$

103 The expected one-step transition reward $q(x, a)$, is defined as

$$105 \quad q(x, a) = \sum_{j=1}^N r_{ij}^a p_{ij}^a. \quad (5)$$

106 The unique solution of the above DPE can be calculated iteratively by the successive approximation method
 107 (Hernandez-Lerma, 1989)⁴:

$$110 \quad v_n(x) = \max_{a \in \mathbf{A}} \left[q(x, a) + \beta \sum_{j=1}^N v_{n-1}(x) p_{ij}^a \right]. \quad (6)$$

111 Therefore, for a specific control problem, once the transition matrix and the reward matrix are defined, then
 112 by maximizing the total expected reward, a policy for choosing an alternative for each state can be obtained.
 113 This represents the optimal strategy that should be followed.

114 3. Traffic dynamics

115 Consider the typical four-legged isolated traffic intersection shown in Fig. 1, where the various possible traf-
 116 fic movements are labeled according to NEMA (National Electrical Manufacturers Association) convention.

² The states of a Markov control model are defined on the Borel space—a Borel subset of a complete separable metric space. The Borel set of a metric space is the set in the smallest Borel field containing the open subset of that metric space. See, e.g., Loeve, M. Probability Theory I, fourth ed., Springer-Verlag, 1977, pp. 92.

³ A function T from S into itself, where (S, d) is a metric space, is a contraction operator if $d(Tu, Tv) \leq \beta d(u, v)$ for $0 \leq \beta < 1$ and $\forall u \in S, v \in S$.

⁴ See Appendix A for proof.

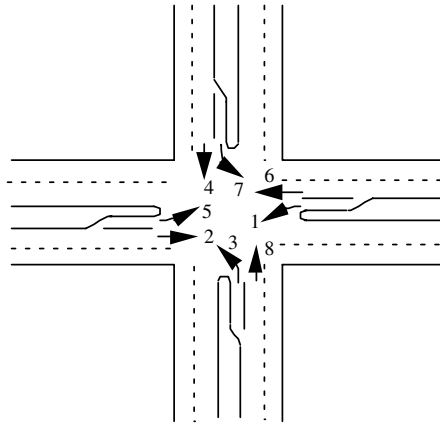


Fig. 1. A typical traffic intersection.

117 The state equation for the continuous traffic flow process associated with any movement j that is sampled
 118 every Δt seconds, where time is indexed with the integer k , can be expressed by the current queue $q^j(k)$:

$$120 \quad q^j(k) = q^j(k-1) + \Delta q^j(k), \quad j = 1, 2, \dots, 8, \quad (7)$$

121 where $\Delta q^j(k) = q_{\text{in}}^j(k) - q_{\text{out}}^j(k)$ is the difference between the input $q_{\text{in}}^j(k)$ and the output $q_{\text{out}}^j(k)$ during time
 122 interval $[k-1, k)$, and $q^j(k-1)$ is the queue at previous time instant $(k-1)$. For a typical four-legged traffic
 123 intersection with eight movements, the current queue $q(k)$ can be further defined by the vector

$$125 \quad \underline{q}(k) = [q^j(k)]' = [q^1(k), q^2(k), \dots, q^8(k)]', \quad (8)$$

126 where prime (') is used to denote transpose. The input $q_{\text{in}}(k)$ and output $q_{\text{out}}(k)$ of the intersection (i.e., num-
 127 ber of vehicles entering/leaving the intersection) can also be similarly defined as vectors of like dimension:

$$129 \quad \underline{q}_{\text{in}}(k) = [q_{\text{in}}^j(k)]', \quad \underline{q}_{\text{out}}(k) = [q_{\text{out}}^j(k)]'. \quad (9)$$

130 The output $q_{\text{out}}(k)$ can further be expressed as a function of the current control of the intersection, $u(k)$, and
 131 the current queue, $\underline{q}(k)$:

$$133 \quad \underline{q}_{\text{out}}(k) = \underline{f}_{\text{out}}(u(k), \underline{q}(k)), \quad (10)$$

134 where $\underline{f}_{\text{out}}(k)$ is also a vector of the same dimension, i.e.,

$$136 \quad \underline{f}_{\text{out}}(k) = [f_{\text{out}}^j(k)]' \quad (11)$$

137 and where the elements $f_{\text{out}}^j(k)$ are determined by

$$139 \quad f_{\text{out}}^j(k) = \begin{cases} \min \left[q^j(k); \frac{\Delta t}{h_{\text{min}}} \right], & u^j(k) = 0, \\ 0, & u^j(k) = 1 \end{cases} \quad (12)$$

140 in which h_{min} is the minimum headway, and $u^j(k)$ is a dichotomous variable indicating the control signal for
 141 the j th movement: $u^j(k) = 0$ denotes that the j th movement has the green signal and $u^j(k) = 1$ indicates a red
 142 signal.

143 Under standard eight-phase dual-ring control (Fig. 2), the barrier divides the eight NEMA phases into two
 144 interlocked groups (rings): east/west and north/south; in each ring, four movements (two through movements
 145 and their corresponding left-turn movements) must be served if there is demand. Although there are $2 \cdot 4! = 48$
 146 different phase sequences available, depending on the traffic demand, the ring and barrier rules restrict the
 147 maximum number of phase transitions in a single cycle to six—a maximum of three distinct phase combina-

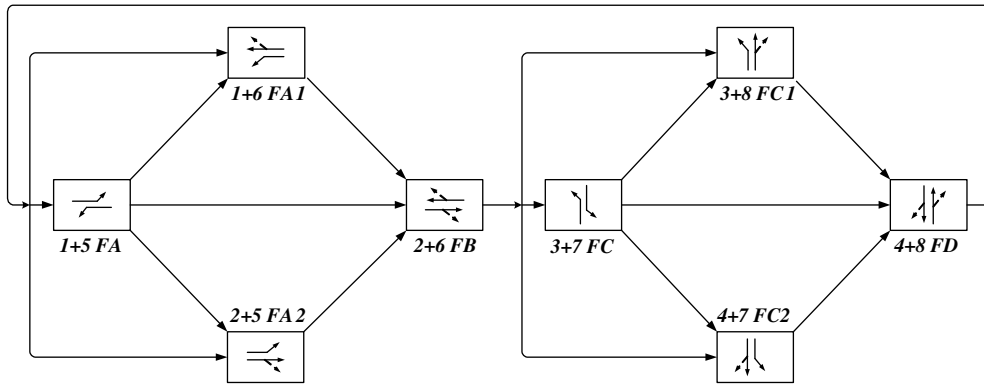


Fig. 2. Eight-phase dual-ring signal control.

148 tions on each side of the barrier. Using this information, the phase sequencing constraints on choice of the
149 current control depends, at most, on three previous control signals:

$$151 \quad u(k) = f_u(q(k), \tau, u(k - \tau_1), u(k - \tau_2), u(k - \tau_3)), \quad (13)$$

152 where τ_1 is the time duration of the most recent previous phase, τ_2 is the time duration of the next-to-last
153 phase, and so on. In addition to the sequencing constraints, the duration of the current signal, τ , must be
154 bounded between some minimum (e.g., minimum green, minimum green extension) and maximum (e.g., max-
155 imum green) time period:

$$157 \quad \tau_{\min} \leq \tau \leq \tau_{\max}. \quad (14)$$

158 This schema easily can be generalized to traffic networks with multiple intersections. In a traffic network
159 with n intersections, the order of the dynamic equations is increased to $n \times 8$ (assuming that there are eight
160 traffic movements in each intersection). However, any complicated traffic network can be decomposed into
161 a group of small “elementary networks”, as shown in Fig. 3, consisting of five intersections. In this manner,
162 the study of the entire traffic network can be reduced to the analysis of these elementary networks and the
163 inter-connections between them.⁵

164 The complete traffic dynamics model for the network shown in Fig. 3 includes the following equations:

165

$$\begin{aligned} \underline{u}(k) &= [\underline{u}_1(k), \underline{u}_2(k), \dots, \underline{u}_5(k)]', \\ \underline{f}_u(k) &= [f_{u1}(k), f_{u2}(k), \dots, f_{u5}(k)]', \\ \underline{q}_{\text{out}}(k) &= [q_{\text{out}1}(k), q_{\text{out}2}(k), \dots, q_{\text{out}5}(k)]', \\ \underline{q}_{\text{in}}(k) &= [q_{\text{in}1}(k), q_{\text{in}2}(k), \dots, q_{\text{in}5}(k)]', \\ \underline{q}(k) &= [q_1(k), q_2(k), \dots, q_5(k)]', \\ \underline{f}_{\text{out}}(k) &= [f_{\text{out}1}(k), f_{\text{out}2}(k), \dots, f_{\text{out}5}(k)]', \\ 167 \quad \underline{q}(k) &= \underline{q}(k-1) + \underline{\Delta}q(k), \end{aligned} \quad (15)$$

168 where

$$170 \quad q_{\text{out}i}^j(k) = f_{\text{out}}(u_i^j(k), q_i^j(k)), \quad (16)$$

⁵ This approach also facilitates parallel processing techniques to improve the computational efficiency for real-time control.

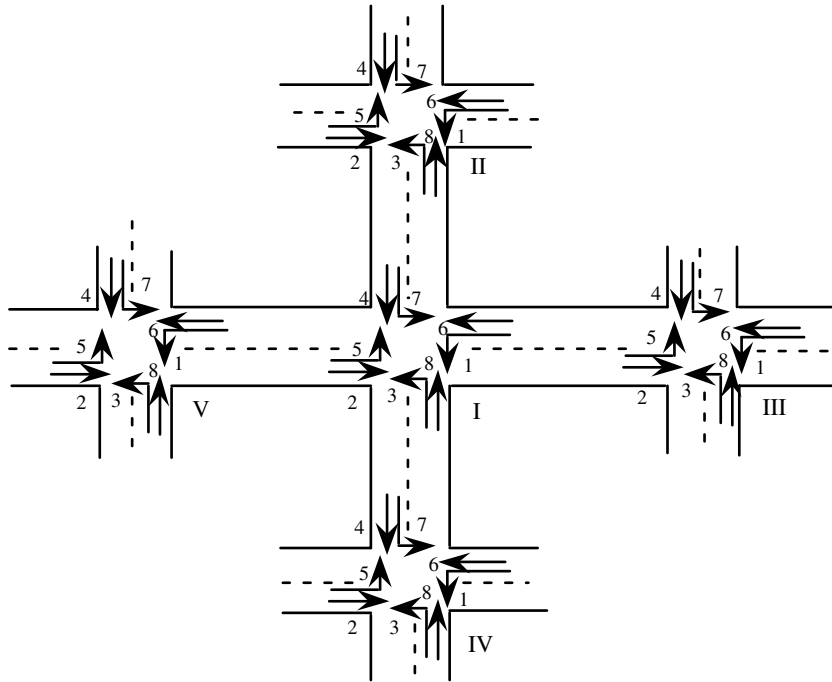


Fig. 3. A typical elementary traffic network with five intersections.

$$f_{\text{out}}^j(k) = \begin{cases} \min \left[q_i^j(k); \frac{\Delta t}{h_{\text{min}}} \right], & u_i^j(k) = 0 \\ 0, & u_i^j(k) = 1 \end{cases} \quad i = 1, 2, \dots, 5; \quad j = 1, 2, \dots, 8. \quad (17)$$

172

173 In Eq. (15), the subscripts to the various vector quantities refer to the particular intersection, and the vector
 174 quantities themselves are as previously defined.

175 Unlike the case of an isolated intersection, the interactions between intersections must be included in the
 176 traffic model for this case. For example, consider the simple case of the two adjacent intersections shown
 177 in Fig. 4.

178 The eight traffic movements associated with each intersection can be classified into two different types:

179 1. *External movement.* The arrival vehicles come from/go to a “dummy node” outside the network (these vehi-
 180 cles can be considered as the “input/output” of this network); and

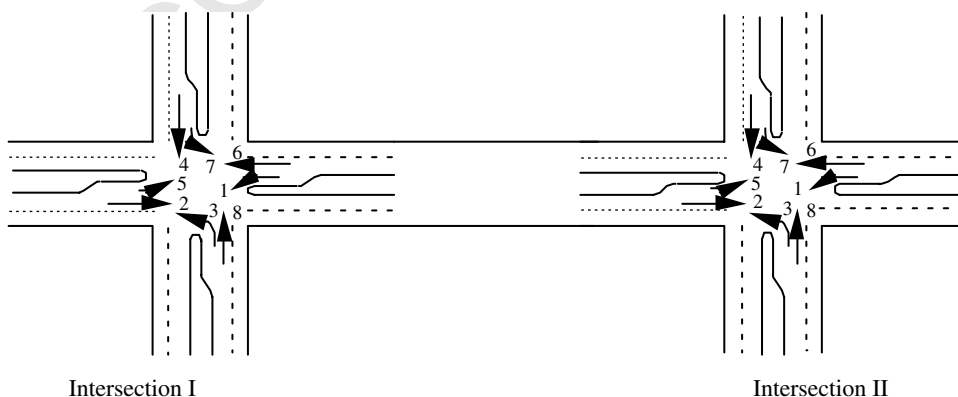


Fig. 4. A traffic network with two intersections.

181 2. *Internal movement.* The arrival vehicles come from/go to a neighboring node inside the network (these vehi-
182 cles can be considered as the “interconnection” of this network).

183

184 For example, movements 1 and 6 are internal movements of intersection I, which receive the outputs from
185 intersection II, movements 3 and 6. All of the other movements of intersection one are external movements.
186 Similarly, all of the movements of intersection II are external movements, with the exception of movements 2
187 and 5, which receive the output from the movements 2 and 7 of intersection I. Then, for intersection I, the
188 internal movements are defined by

$$\begin{aligned} q_{inI}^1(k) &= f_{in} \left(\beta_{II,I}^{3,1} (k - T_{II,I}^3), q_{outII}^3 (k - T_{II,I}^3), \beta_{II,I}^{6,1} (k - T_{II,I}^6), q_{outII}^6 (k - T_{II,I}^6) \right), \\ q_{inI}^6(k) &= f_{in} \left(\beta_{II,I}^{3,6} (k - T_{II,I}^3), q_{outII}^3 (k - T_{II,I}^3), \beta_{II,I}^{6,6} (k - T_{II,I}^6), q_{outII}^6 (k - T_{II,I}^6) \right), \end{aligned} \quad (18)$$

191 where $\beta_{i_1, j_2}^{i_1, j_2}$ is defined as the vehicle turning fraction from intersection i_1 , movement j_1 to intersection i_2 , move-
192 ment j_2 ,⁶ and where $T_{i_1, i_2}^{j_1}$ represents the travel time for the first vehicle in the platoon of vehicles in movement j_1
193 of intersection i_1 to reach intersection i_2 .

194 The time-dependent turning factors can be represented by the turning fraction matrix, $\underline{\beta}(k)$, whose elements
195 indicate the percentage of vehicles turning from a certain movement at the upstream intersection to a specific
196 movement at the down stream intersection. For the case of two intersections shown in Fig. 4, $\underline{\beta}(k)$ can be writ-
197 ten as a 16×16 matrix:

$$\underline{\beta}(k) = \begin{bmatrix} \underline{0} & \left[\beta_{I,II}^{i_1, j_2}(k) \right] \\ \left[\beta_{II,I}^{i_1, j_2}(k) \right] & \underline{0} \end{bmatrix} = \begin{bmatrix} \underline{0} & \underline{\beta}_{I,II}(k) \\ \underline{\beta}_{II,I}(k) & \underline{0} \end{bmatrix}, \quad (19)$$

200 where

$$\underline{\beta}_{I,II}(k) = \begin{bmatrix} 0 & 0 & 0 & 0 & 0 & 0 & 0 & 0 \\ 0 & \beta_{I,II}^{2,2}(k) & 0 & 0 & \beta_{I,II}^{2,5}(k) & 0 & 0 & 0 \\ 0 & 0 & 0 & 0 & 0 & 0 & 0 & 0 \\ \dots & & & \dots & & & & \dots \\ 0 & 0 & 0 & 0 & 0 & 0 & 0 & 0 \\ 0 & \beta_{I,II}^{7,2}(k) & 0 & 0 & \beta_{I,II}^{7,5}(k) & 0 & 0 & 0 \\ 0 & 0 & 0 & 0 & 0 & 0 & 0 & 0 \end{bmatrix},$$

$$\underline{\beta}_{II,I}(k) = \begin{bmatrix} 0 & 0 & 0 & 0 & 0 & 0 & 0 & 0 \\ 0 & 0 & 0 & 0 & 0 & 0 & 0 & 0 \\ \beta_{II,I}^{3,1}(k) & 0 & 0 & 0 & 0 & \beta_{II,I}^{3,6}(k) & 0 & 0 \\ 0 & 0 & 0 & 0 & 0 & 0 & 0 & 0 \\ 0 & 0 & 0 & 0 & 0 & 0 & 0 & 0 \\ \beta_{II,I}^{6,1}(k) & 0 & 0 & 0 & 0 & \beta_{II,I}^{6,6}(k) & 0 & 0 \\ 0 & 0 & 0 & 0 & 0 & 0 & 0 & 0 \\ 0 & 0 & 0 & 0 & 0 & 0 & 0 & 0 \end{bmatrix}.$$

202

203 Using this general expression for $\underline{\beta}(k)$

204

$$206 \quad q_{in_i}^j(k) = f_{in} \left(\beta_{m,i}^{r,j}(k - T_{m,i}^r), q_{out_m}^r(k - T_{m,i}^r) \quad \forall r \in M_m^i, m \in I_i \right), \quad (20)$$

⁶ For example, $\beta_{II,I}^{3,1}(k)$ represents the percentage of vehicles from movement 3 of intersection II turning to movement 1 of intersection I during time interval k .

207 where I_i is the set of all neighboring intersections with direct approaches to intersection i , and M_m^i is the set of
 208 all movements of intersection m that contribute to the internal movements of intersection i .

209 Practical application of Eq. (20) relies on the ability to predict both the time-dependent turning fractions,
 210 $\beta(k)$, and the platoon travel times from neighboring intersections to the target intersection, T_{i_1, i_2}^j . The estima-
 211 tion of turning fractions from count data has been the subject of numerous investigations; see, e.g., the review
 212 provided by Maher (1984) for a summary of models that require counts for only one cycle but need prior turn-
 213 ing proportion estimation. However, the accuracy of such methods is highly dependent on how representative
 214 the *a priori* estimates are of the current events. Alternatively, estimations based on simple time-series analyses
 215 do not need such prior estimates but require a long time frame which impedes their responsiveness, and are
 216 unreliable during times of sudden and highly irregular turning movement changes caused by such unforeseen
 217 events as traffic accidents. Davis and Lan (1995) have proposed a method that estimates intersection turning
 218 movement proportions from less-than-complete sets of traffic counts, even under conditions in which the num-
 219 ber or placement of detectors does not support complete counting. Chang and Tao (1997) propose a time-
 220 dependent turning estimation that incorporates signal timing parameters on the distribution of intersection
 221 flows. More recently, Mirchandani et al. (2001) propose four closed-form estimation methods: (1) maximum
 222 entropy (ME), (2) generalized least-squared (GLS), (3) least-squared error (LS), and (4) least-squared error/
 223 generalized least-squared error (LS/GLS). Although not specifically addressing the estimation of turning frac-
 224 tions for purposes of signal timing, Chen et al. (2005) and Nie et al. (2005) have examined a generalized path
 225 flow estimator (PFE) as a one-stage network observer to estimate path flows and path travel times from traffic
 226 counts in a transportation network, and have shown it to be a reasonably accurate method for estimating
 227 dynamic path flows based on limited real-time detector data. The estimated path flows can further be aggre-
 228 gated to obtain dynamic origin–destination (O–D) flows, a by-product of which are the turning fractions at the
 229 various nodes in the network. In the results presented here, we presume that the $\beta(k)$ can be determined from
 230 one or another of these existing estimation procedures.

231 In order to determine the platoon travel times from neighboring intersections to the target intersection,
 232 T_{i_1, i_2}^j , we employ the well-known empirical model developed by Robertson (1967) for platoon dispersion to
 233 describe the flow dynamics from upstream intersections to downstream movements. Robertson's dispersion
 234 model has been used and tested extensively in field applications involving both TRANSYT and SCOOT,
 235 and found to be a very effective representation of platoon dynamics. In its basic form, the model has the
 236 representation:

$$238 \quad Q_1(t_0 + T) = F \cdot Q_2(t_0) + (1 - F) \cdot Q_1(t_0 + T - 1), \quad (21)$$

239 where

$$241 \quad F = \frac{1}{1 + \alpha\beta T_{\text{avg}}}$$

242 and where Q_1, Q_2 are the traffic volumes at the downstream and upstream intersections (measured in vehicles/
 243 h), respectively; α and β are called platoon dispersion parameters; t_0 is the initial time when the platoon leaves
 244 the upstream intersection; T_{avg} is the average travel time, and T is the minimum travel time between the two
 245 intersections, i.e., the time for the lead vehicle in the platoon to reach the downstream intersection.⁷ T is re-
 246 lated to T_{avg} through the parameter β , i.e.,

$$249 \quad T = \beta T_{\text{avg}}. \quad (22)$$

250 Substituting Robertson's platoon dispersion formula into Eq. (20) leads to

$$252 \quad q_{\text{in}i}^j(k) = \sum_{\substack{\forall r \in M_m^i \\ m \in I_i}} F \cdot \beta_{m,i}^{r,j}(k - T_{m,i}^r) \cdot q_{\text{out}m}^r(k - T_{m,i}^r) + (1 - F) \cdot q_{\text{in}i}^j(k - 1) \quad (23)$$

253 with the current control vector defined by

$$255 \quad u_i(k) = f_u(q_i(k), \tau_i, u_i(k - \tau_1), u_i(k - \tau_2), u_i(k - \tau_3)), \quad (24)$$

⁷ Both T and T_{avg} must be rounded to integer values.

256 where $\tau_{\min i} \leq \tau_i \leq \tau_{\max i}$, $\beta_{m,i}^{r,j}(\cdot)$ can be derived from counts from upstream stopline detectors according to
 257 existing procedures discussed previously, and where the $T_{m,i}^r$ are determined by Eq. (22) from parameter spec-
 258 ification and average travel speed.

259 4. Markov adaptive control model for traffic signal control

260 The state variable in the traffic dynamics equation developed above is queue length. Although the state of
 261 the Markov control model can be defined as the number of vehicles in the intersection, this approach results in
 262 an excessively large number of states, even for a single intersection.⁸ To address this problem, the state of the
 263 Markov control model is instead defined by introduction of a binary threshold value (number of vehicles) indi-
 264 cating whether or not the current queue for a particular movement is sufficiently large to be “congested”, i.e.,
 265 if the queue length of a specific movement is greater than its threshold value, then the movement is in the “con-
 266 gested mode”; otherwise it is in the “non-congested mode”. These binary modes (congestion/non-congestion)
 267 are defined as the two states in the state space \mathbf{X} .⁹

268 Since the state space is discrete, the probability measure \mathbf{P} is a discrete transition law, and the probability
 269 matrix \mathbf{P} is time-varying due to the time-varying traffic flow. At time step k , \mathbf{P} is a function of $q(k)$, $\Delta\hat{q}(k+1)$,
 270 and $\underline{u}(k)$:

$$272 \quad \mathbf{P}(k) = f_p[q(k), \underline{q}_{\text{in}}(k+1), u(k)], \quad (25)$$

273 where $q(k)$ is the current queue, $\Delta\hat{q}(k+1)$ is the estimated number of arrivals in the next time interval, and
 274 $\underline{u}(k)$ is the control signal. Assuming that at time step k , the current queue length of a specific movement i
 275 is denoted by q_0 ; and q_g vehicles can pass through the intersection if the traffic signal for this movement is
 276 green; then the transition probability from any current state (either congested or non-congested) to the
 277 non-congested state under control signal u can be written as

$$279 \quad p_{S_i \rightarrow N_i}^u = p\left(\hat{q}_{\text{in}}^i + q_0^i - \delta(u_i) \cdot q_g^i \leq q_{\text{threshold}}^i\right) \quad (26)$$

280 and, to the congested state, as

$$282 \quad p_{S_i \rightarrow C_i}^u = 1 - p_{S_i \rightarrow N_i}^u, \quad (27)$$

283 where

$$285 \quad \delta(u_i) = \begin{cases} 1, & \text{when } u_i = G_i, \\ 0, & \text{otherwise.} \end{cases} \quad (28)$$

286 In the above, $q_{\text{threshold}}^i$ is the threshold which defines the congested/non-congested state; S_i is the current state
 287 (N_i for non-congested state and C_i for congested state); u_i is the control signal (G_i for green signal and R_i for
 288 red signal). Two special cases are noted in that:

$$290 \quad p_{C_i \rightarrow C_i}^{R_i} \equiv 1, \quad \text{and} \quad p_{C_i \rightarrow N_i}^{R_i} \equiv 0. \quad (29)$$

291 As mentioned previously, for a typical traffic intersection with eight independent movements, the total number
 292 of states is $2^8 = 256$. The transition probability for each movement is also independent; therefore, the overall
 293 transition probability for an intersection is

$$295 \quad P_{\text{State}_j \rightarrow \text{State}_r}^u = \prod_{i=1}^8 p_{S_i \rightarrow S_i}^u, \quad (30)$$

296 where $j, r = 1, 2, \dots, 256$; and $\underline{u}(k) = [u_1, u_2, \dots, u_8]^T$.

⁸ For example, if the number of vehicles under consideration is 20 per movement, then for an isolated intersection with eight movements, the total number of states is $21^8 \approx 3.78 \times 10^{10}$.

⁹ For an isolated intersection with eight movements and ten vehicles per movement, the number of states is dramatically reduced by a factor of 10^8 to $2^8 = 256$.

297 The reward matrix \mathbf{R} has the same dimension and a definition similar to that of the probability matrix. The
 298 control objective is to maintain the non-congested condition or, if already congested, to transit to a non-con-
 299 gested state. The latter yields a greater reward than the former and the transition from a non-congested state
 300 to congested carries a greater penalty than remaining in a congested state. Since the congested/non-congested
 301 state is defined in terms of queue length, the reward matrix is a function of the current queue, the threshold,
 302 and the control signal:

$$304 \quad \mathbf{R}(k) = f_r[q_0(k), q_{\text{threshold}}(k), \mathbf{u}(k)]. \quad (31)$$

305 For example, if the objective is to minimize the queue length, then the reward for each possible case can be
 306 chosen as the following:

$$r_{N_i \rightarrow N_i}^{G_i} = q_0^i + M_1,$$

$$r_{N_i \rightarrow N_i}^{R_i} = q_0^i + M_2,$$

$$r_{N_i \rightarrow C_i}^{G_i} = q_0^i + M_3,$$

$$r_{N_i \rightarrow C_i}^{R_i} = M_4,$$

$$r_{C_i \rightarrow N_i}^{G_i} = q_0^i + M_5,$$

$$r_{C_i \rightarrow N_i}^{R_i} = N.A.,$$

$$r_{C_i \rightarrow C_i}^{G_i} = q_0^i + M_6,$$

$$308 \quad r_{N_i \rightarrow N_i}^{R_i} = M_7,$$

309 where M_i , $i = 1, 2, \dots, 7$, are constants which can be specified for a specific traffic control problem.¹⁰

310 Similar to the probability matrix, the overall reward for an intersection with eight independent movements
 311 is

$$314 \quad r_{\text{State}_j \rightarrow \text{State}_r}^{\mathbf{u}} = \prod_{i=1}^8 r_{S_i \rightarrow S_i}^{M_i}, \quad (32)$$

315 where $j, r = 1, 2, \dots, 256$.

316 The signal phases are the different alternatives for each state; for a typical isolated traffic intersection with
 317 eight independent movements under eight-phase dual-ring signal, the signal control problem takes the form of
 318 a 256-state Markov process with eight alternatives for each state. The optimal policy is then obtained by
 319 selecting the alternative for each state that maximizes the total expected reward. As has been demonstrated
 320 above, this optimal solution is unique and can be calculated iteratively by the successive approximation
 321 method.

322 The proposed Markov control model can be illustrated by the simplified example of the two-phase isolated
 323 intersection shown in Fig. 5, in which traffic flows along two directions, i.e., north/south (denoted by 1) and
 324 east/west (denoted by 2). Thus, there are four possible states, i.e., N_1N_2 , N_1C_2 , C_1N_2 , and C_1C_2 . Fig. 6 shows
 325 the schematics of this Markov chain. To simplify the example, amber displays and all red signals (R_1R_2) are
 326 ignored; G_1G_2 is prohibited for obvious reasons. Under these conditions, there are two alternatives (signal
 327 phases) in each state, i.e., G_1R_2 and R_1G_2 . With the usual assumption of Poisson arrivals, the various transi-
 328 tion probabilities can be calculated directly. For example, the transition probabilities from the non-congested
 329 state are

$$p_{N \rightarrow N}^G = \sum_{n=1}^{q_{\text{threshold}} - q + q_g} \frac{(\lambda \Delta t)^n e^{-\lambda \Delta t}}{n!}, \quad p_{N \rightarrow N}^R = \sum_{n=1}^{q_{\text{threshold}} - q} \frac{(\lambda \Delta t)^n e^{-\lambda \Delta t}}{n!}, \quad (33a)$$

$$331 \quad p_{N \rightarrow C}^G = 1 - p_{N \rightarrow N}^G, \quad p_{N \rightarrow C}^R = 1 - p_{N \rightarrow N}^R, \quad (33b)$$

332 where n is a positive integer ($n = 1, 2, \dots$); λ is the average vehicle arrival rate (vehicles/h) and Δt is the time
 333 interval (i.e., duration of each counting period).

¹⁰ If the objective is to minimize the delay time, the specific rewards can also be chosen as functions of the vehicle delay.

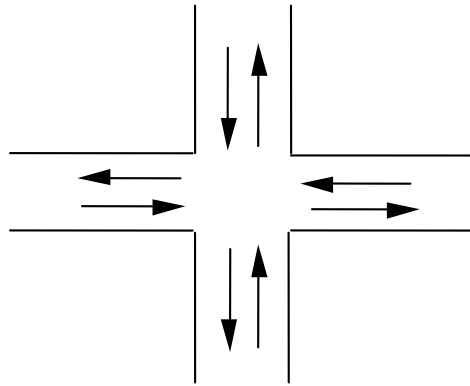


Fig. 5. An isolated intersection with through movements only.

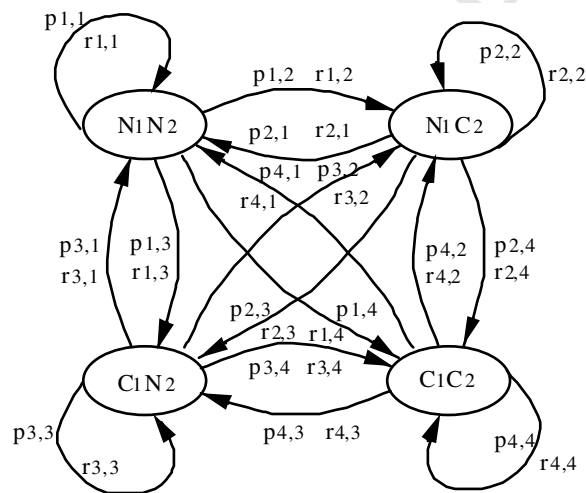


Fig. 6. The Markov chain for the example.

334 The corresponding state probabilities are

$$\begin{aligned} P_{N_1N_2 \rightarrow N_1N_2}^{G_1R_2} &= P_{N_1 \rightarrow N_1}^{G_1} \cdot P_{N_2 \rightarrow N_2}^{R_2}, \\ P_{N_1N_2 \rightarrow N_1C_2}^{G_1R_2} &= P_{N_1 \rightarrow N_1}^{G_1} \cdot P_{N_2 \rightarrow C_2}^{R_2}, \end{aligned} \quad (34)$$

336 \vdots

337 Since, for this example, there are four states with two alternatives for each state, the elements above form
 338 an 8×4 transition probability matrix, as shown in Table 1. Elements of the reward matrix can be calculated in
 339 similar fashion.

340 A general block diagram of traffic control using this scheme at an isolated signalized intersection is illus-
 341 trated in Fig. 7, and a corresponding computational flow chart shown in Fig. 8. Based on the current and
 342 the estimated traffic flow, the controller generates a traffic control signal to control the traffic system for
 343 the next time interval.

344 In the application of this procedure to real-time adaptive control for a traffic system, the time-varying prob-
 345 ability matrix \mathbf{P} and the reward matrix \mathbf{R} are calculated and updated every Δt seconds¹¹; a decision is then

¹¹ The minimum time interval is chosen as $\Delta t = \tau_{\min}$ (i.e., minimum green extension time).

Table 1

The state probability matrix for the example

| State | | N_1N_2 | N_1C_2 | C_1N_2 | C_1C_2 |
|----------|----------|--|--|----------|--|
| N_1N_2 | G_1R_2 | $P_{N_1N_2 \rightarrow N_1N_2}^{G_1R_2}$ | $P_{N_1N_2 \rightarrow N_1C_2}^{G_1R_2}$ | ... | $P_{N_1N_2 \rightarrow C_1C_2}^{G_1R_2}$ |
| | R_1G_2 | $P_{N_1N_2 \rightarrow N_1N_2}^{R_1G_2}$ | | | |
| N_1C_2 | G_1R_2 | | ... | | |
| | R_1G_2 | | | | |
| C_1N_2 | G_1R_2 | | | ... | |
| | R_1G_2 | | | | |
| C_1C_2 | G_1R_2 | | | | $P_{C_1C_2 \rightarrow C_1C_2}^{G_1R_2}$ |
| | R_1G_2 | | | | $P_{C_1C_2 \rightarrow C_1C_2}^{R_1G_2}$ |

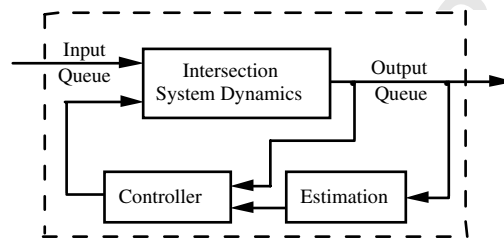


Fig. 7. Traffic control at signalized intersection.

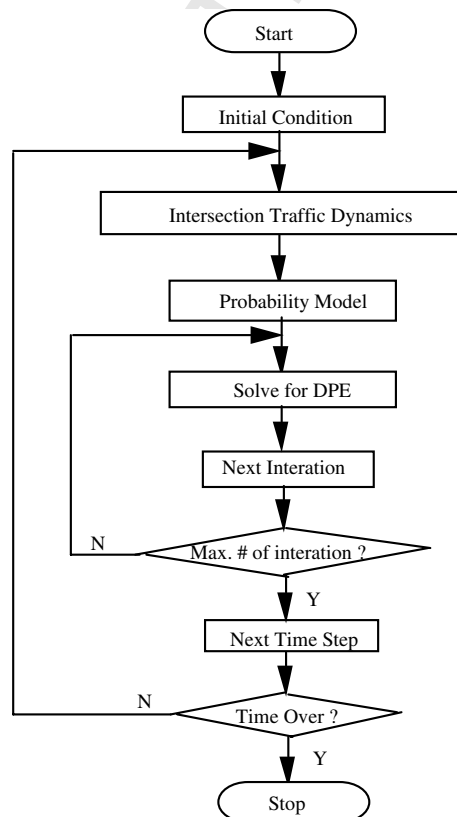


Fig. 8. Computational flow chart.

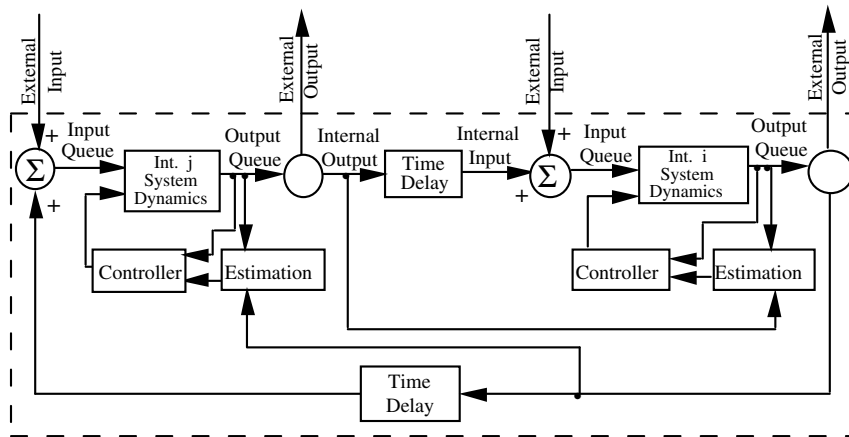


Fig. 9. Traffic control for two intersections.

346 made regarding the choice of the control signal for the next time interval based on the current measurement
 347 from the detector, as well as the estimation. Once the optimal policy is found, it is implemented for one time
 348 step (i.e., Δt seconds). At the next time interval, both the probability matrix and reward matrix are updated
 349 and the whole decision-making process is repeated.

350 To enforce the phase constraints, a step-by-step decision-making procedure (also termed a “decision tree”)
 351 is employed. For example, a decision is made first to determine which ring will be served by the Markovian
 352 decision algorithm. After this is determined, the second decision is to choose one of the four alternatives from
 353 the first decision, again using the Markovian decision algorithm. The next phase is either fixed or can be cho-
 354 sen from the two phases left, depending upon the second decision. At the last decision step for this ring, there
 355 is either no phase or just one fixed phase left. This procedure not only guarantees the phase constraints but
 356 also dramatically reduces computation time.

357 Application of the decision control to the signal control of a network of multiple intersections proceeds
 358 along a similar manner; a block diagram for the control system of two traffic intersections is shown in
 359 Fig. 9. In such cases, the control signal of the two neighboring intersections do not interact until some min-
 360 imum travel time, at which time the control is modeled through the probability estimation of internal move-
 361 ment arrivals at the downstream intersections. That is, assuming that the minimum travel time between two
 362 intersections is longer than the minimum green extension time, the control signals of the two intersections do
 363 not interact due to the random travel time delay between them. After the minimum travel time, the control at
 364 one intersection does affect intersections downstream; this effect is modeled in the probability estimation at the
 365 downstream intersections. As a result, adjacent intersections can be “isolated” and the respective control
 366 actions can be calculated separately.

367 5. Results on application of Markov adaptive signal control model

368 In this section, the control model is tested by simulation on both an isolated traffic intersection and a typical
 369 traffic network with five interconnected intersections to evaluate its performance with respect to conventional
 370 full-actuated control. Specifically, a series of computer simulations are performed, under various different
 371 vehicle arrival rates, and the means and variances of the respective performance measures of the conventional
 372 and proposed adaptive control algorithm are analyzed. The simulations assume that queues on all approaches
 373 are empty as an initial condition and that vehicle arrivals on external approaches follow a Poisson distribu-
 374 tion; for demonstration purposes, a value of $q_{\text{threshold}} = 1$ (i.e., the presence of any queue) was assumed.
 375 The reward matrix was based on the objective being to minimize the queue length, and the reward calculated
 376 according to Eq. (32). In the case of the network simulation, the distance between any two adjacent intersec-
 377 tions is chosen to be 1000 feet. The parameters used in the simulation (for all the movements) are summarized
 378 as follows:

| Parameter | Value |
|-------------------------------|-------|
| Minimum green time (s) | 3 |
| Maximum green time (s) | 30 |
| Extension (gap) time (s) | 3 |
| Yellow time (s) | 3 |
| All red time (s) | 0 |
| Loss time (s) | 0 |
| Minimum departure headway (s) | 2 |
| Minimum arrival headway (s) | 2 |

379 Using the same set of input (arrival) data, the Markovian control algorithm and the conventional full-actu-
 380 ated control were applied to a four-legged isolated traffic intersection, such as that shown in Fig. 1, with eight
 381 movements (four through movements and their corresponding left-turn movements) to evaluate their perfor-
 382 mances. The algorithm used to simulate full-actuated control was designed to mimic the logic of a common
 383 Type 170 dual ring controller with parameters as specified in the previous table—eight-phase operation was
 384 assumed. To minimize initial condition effects, the two algorithms are applied for a simulated time of
 385 65 min, and the average delay (per vehicle) during the last five minutes of the simulation is used for compar-
 386 ison.¹² Two different general cases were considered: (1) uniform (balanced) demand among all conflicting
 387 movements, and (2) the through traffic demand dominates the left-turn demand by a ratio of 2:1. The two
 388 algorithms were applied for different arrival rates, representing a range of both unsaturated and saturated con-
 389 ditions. (Under the assumption of 2-second minimum headways, the intersection has a total capacity of 3600
 390 vehicles per hour of green.) In order to provide statistical significance for the simulation results, the two algo-
 391 rithms were tested on different sets of random data for each arrival rate (a total of forty in the cases in which
 392 left-turning traffic was assumed equal to through traffic, and fifteen in the cases in which left-turning traffic
 393 was equal to half of the through traffic).

394 The means of the average delay per vehicle for the final five-minute period of each set of forty simulations
 395 corresponding to the two cases of left-turn to through traffic ratios of 1.0 (LT/T = 1.0) and 0.5 (LT/T = 0.5)
 396 are plotted in Fig. 10, where “MAC” stands for the Markov adaptive control algorithm, and “FAC” stands
 397 for the full-actuated control. As a further “benchmark” comparison, delay calculations based on Webster’s
 398 delay equation for Poisson arrivals under fixed-time (pre-timed) control are also provided (labeled Pre
 399 ($C = 60$ s) and Pre ($C = 45$ s) for cycle lengths of 60 and 45 s, respectively).

400 Significance tests based on t -statistics resulting from hypothesis tests on the difference of sample means indi-
 401 cate that the difference in means of the simulation results is significantly different (at 0.05 level or above) for all
 402 cases except for the LT/T = 1.0 case in which the total intersection volume is 1500 vph. The hypothesis tests on
 403 the difference of means assume that the two populations are independent and have a normal distribution. Alter-
 404 natively, order statistics (distribution-free statistics) estimate the limits within which a certain percentage of the
 405 probability of the random variable lies with a certain degree of confidence without having prior knowledge of
 406 the probability distribution. For the case involving 40 samples taken from a population, the upper/lower bound
 407 within which 90% of the probability of the random variable lies can be obtained with 92% confidence. Fig. 11
 408 displays these bounds on the steady state delay resulting both from full-actuated and from Markovian control
 409 algorithms.

410 From the above figures, except for the case in which the left-turn traffic volume is equal to the through vol-
 411 ume (LT/T = 1.0) and the traffic volume is relatively light (e.g., arrival rate is 200 vehicles/hour/movement),
 412 the performance of the Markov algorithm is significantly better than the fully actuated controller (as well as
 413 the pre-timed controller). For example, for LT/T = 1.0, when $\lambda = 300$, the Markov algorithm shows about a
 414 25% improvement on the average steady state delay; for $\lambda = 400$ and $\lambda = 500$, the average steady state delay of
 415 the Markov controller is only about one half of that of the full-actuated controller. As expected, under sat-
 416 urated conditions both algorithms exhibit increasingly worse delays, although the Markov control (on aver-

¹² In most cases, the steady state is reached within an hour of simulation.

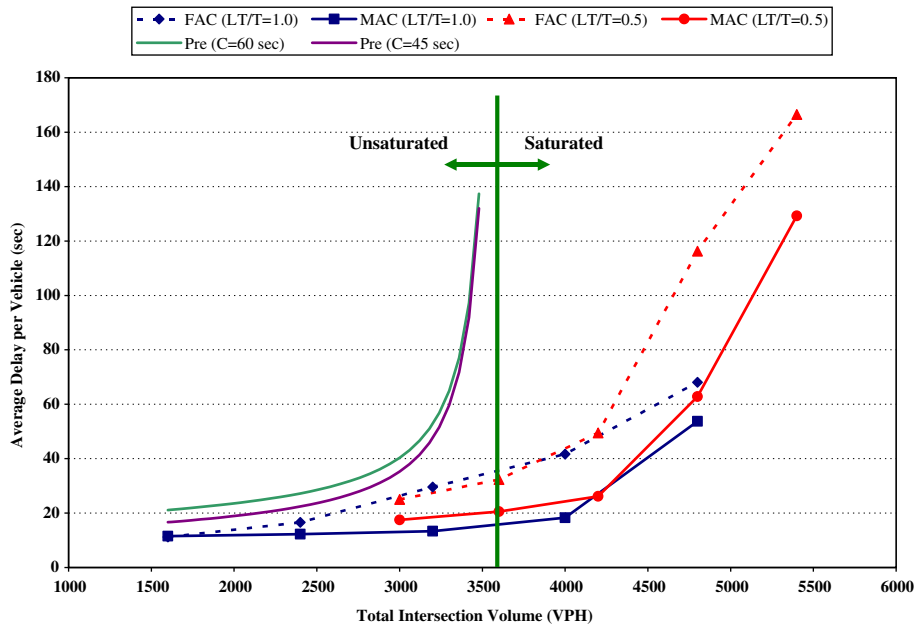


Fig. 10. Algorithm performance comparison for isolated intersection.

age) still outperforms full-actuated control. The simulation results indicate that by applying the Markov adaptive control algorithm, the average delay at an isolated intersection may be reduced dramatically (22–51%).

The Markov adaptive control algorithm was also tested on a typical traffic network of five intersections, such as that depicted in Fig. 3. For this case, Poisson arrivals were assumed at the external inputs; the arrivals at all internal approaches are an outcome of the control strategy employed at associated upstream intersections. The tests were conducted for $LT/T = 1.0$ using five different arrival rates: $\lambda = 200, 300, 400, 500$ and 600 vehicles per hour per movement. The internal approaches linking the five intersections were assumed to be 1000 ft in length, and the average travel speed assumed to be 30 mph (resulting in a value of $T_{avg} = 23$ s). The parameters in Robertson's platoon dispersion model were assumed to be $\alpha = 0.35, \beta = 0.8$ —the common default values for US studies. The mean values (of the 40 sets of data) of the steady state delay are plotted in Fig. 12. The dotted lines in Fig. 12 display the upper/lower bounds within which 90% of the probability of the steady state delay resulting both from full-actuated and from Markovian control algorithms lay.

The results indicate that the Markov algorithm substantially outperforms traditional full-actuated control, particularly when the intersection is at, or near saturation. For example, when $\lambda \leq 500$ (total intersection volume of 4000 vph), the average steady state delay of the Markov controller is only about one half of that of the fully actuated controller. Under heavy over-saturated conditions ($\lambda = 600$), delay with both algorithms tend to converge at a relatively high value.

We note that, under simple five-node network conditions with identical arrival rates, the performance of the Markov control algorithm closely mirrors that obtained in the case of the isolated intersection example (Fig. 13). Although preliminary, the results suggest that application of the algorithm in a network setting tends to decrease variability in performance; this is expected, since the variability expressed in the Poisson arrival patterns at the external nodes becomes an increasingly minor factor as the number of internal approaches increases. This latter factor may help to explain the large variance seen in the isolated intersection case under heavy oversaturation.

As stated previously, the specific objective used in these examples of application of the Markov Adaptive Control algorithm was not specifically to minimize delay, but rather to minimize the queues on the intersection approaches; the delay performance characteristics presented above were an ancillary outcome of the specific objective. Relative to performance related to that specific objective, Fig. 14 presents representative values of

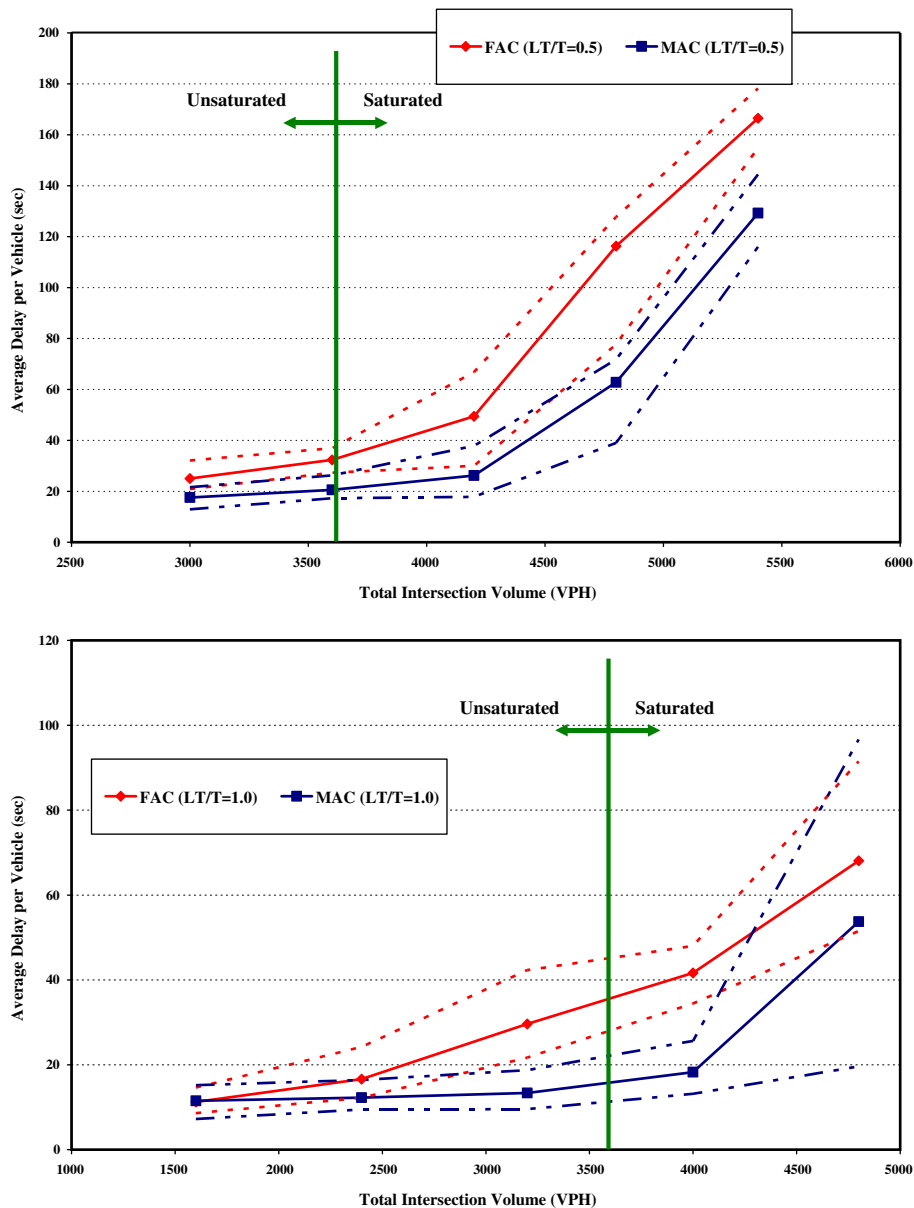


Fig. 11. Upper and lower bounds on simulation results.

445 the maximum queues for each movement obtained for the network case in which the total intersection volume
 446 is 3200 vph, or about 90% of intersection capacity.

447 The results indicate that the Markov Adaptive Control algorithm significantly outperforms full-actuated
 448 control in this aspect, although it must be noted that full-actuated control is not explicitly designed to mini-
 449 mize queue length, but rather implicitly works toward this end via its extension settings.

450 6. Summary and conclusions

451 Traffic signal control is a major ATMS component and its enhancement arguably is the most efficient way
 452 to reduce surface street congestion. The objective of the research presented here has been to present a more
 453 effective systematic approach to achieve real-time adaptive signal control for traffic networks.

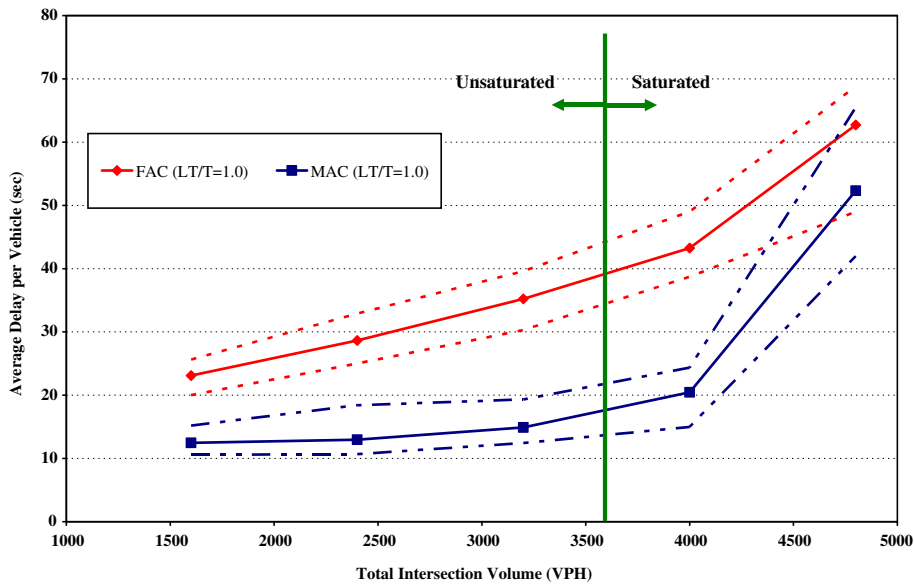


Fig. 12. Algorithm performance comparison for simple network case.

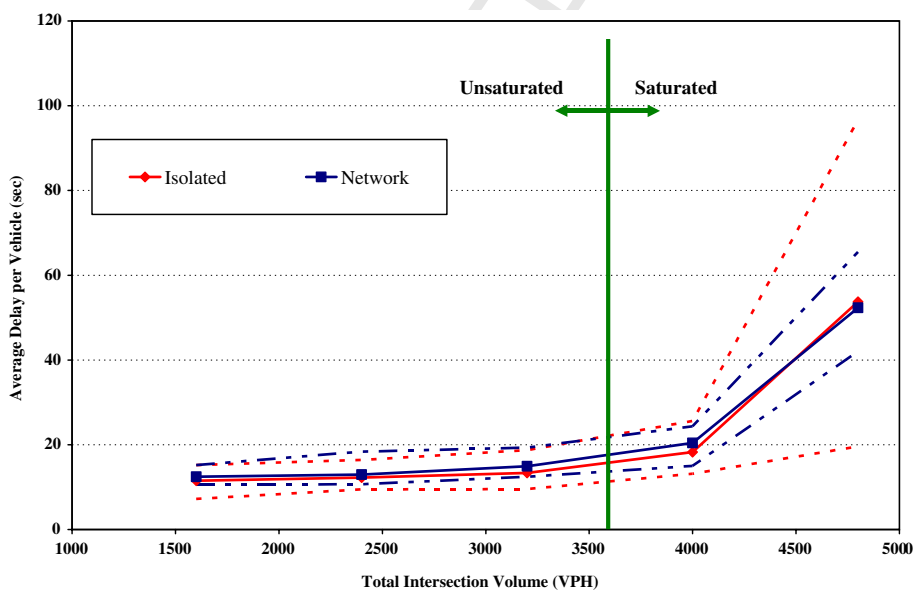


Fig. 13. MAC performance comparison between network and isolated intersection examples.

454 In this research, the problem of finding optimal traffic signal timing plans has been solved as a decision-
 455 making problem for a controlled Markov process. Controlled Markov processes have been used extensively
 456 to analyze and control complicated stochastic dynamical systems; its probabilistic, decision-making features
 457 match almost perfectly with the design features of a traffic signal control system. The Markovian model devel-
 458 oped herein as the system model for signal control incorporates Robertson's platoon dispersion traffic model
 459 between intersections and employs the value iteration algorithm to find the optimal decision for the controlled
 460 Markov process. Analysis of computer simulation results indicates that this systematic approach is more effi-
 461 cient than the traditional full-actuated control, especially under the conditions of high traffic demand.

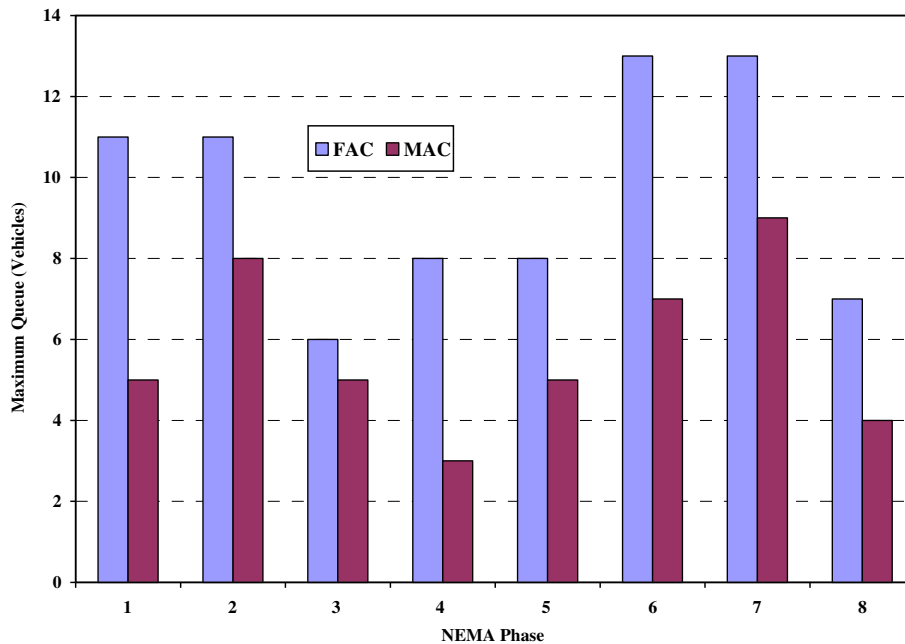


Fig. 14. Maximum queue comparison (3200 vph).

462 There are, of course, significant limitations to the present approach. Most notable is that as the size of the
 463 traffic network increases, i.e., the number of nodes/intersections and/or links increases, the dimension of the
 464 Markovian control model increases dramatically, requiring more memory space and computation time. This
 465 dimensionality issue is very important to real-time implementation, where processing speed is crucial. In the
 466 current formulation, one potential solution to this problem is alluded to by decomposing the network into sets
 467 of inter-linked network kernels of five intersections that could be handled by distributed/parallel processing
 468 protocols; however, no attempt has been made to thoroughly investigate the issues of such decomposition
 469 algorithms. Further, before any attempt to implement the results, a comprehensive sensitivity analysis needs
 470 to be conducted to study the effect of the various parameters employed in the simulation testing on both the
 471 performance of the model as well as on the objective function. Finally, for field testing, the original C language
 472 code must first be rewritten into assembly language; then the firmware can be loaded, or "burned in" to the
 473 PROM (Programmable Read-Only Memory) chip of the controller.

474 7. Uncited reference

475 [Hernandez-Lerma and Lasserre \(1996\).](#)

476 Appendix A. Successive approximation method—value iteration algorithm

477 The successive approximation algorithm given by Eq. (6) can be proved by Banach's fixed point theorem.
 478 Banach's fixed point theorem states that if T is a contraction operator mapping a complete metric space
 479 (S, d) into itself, then T has a unique fixed point v^* such that for any $v \in S$ and $n \geq 0$:

$$481 \quad d(T^n v, v^*) \leq \beta^n d(v, v^*), \quad (\text{A.1})$$

482 where $v^* \in S$ satisfies $Tv^* = v^*$, d is the metric and $0 \leq \beta < 1$.

483 To prove the operator T defined in Eq. (4) for the Markov process is a contraction operator, let $B(X)$ be the
 484 Banach space (a complete normed linear space) of real-valued bounded measurable functions on a Borel space
 485 X with supremum norm:

$$487 \quad \|v\| = \sup_x |v|. \quad (\text{A.2})$$

488 For any $u \in B(X)$ and $v \in B(X)$, we have

$$490 \quad \begin{aligned} |Tv(x) - Tu(x)| &= \left| \max_{a \in A} \left[q(x, a) + \beta \sum_{j=1}^N v(x) p_{ij}^a \right] - \max_{a \in A} \left[q(x, a) + \beta \sum_{j=1}^N u(x) p_{ij}^a \right] \right| \\ &\leq \beta \max_{a \in A} \left| \sum_{j=1}^N [v(x) - u(x)] p_{ij}^a \right| \leq \beta \|v(x) - u(x)\|. \end{aligned}$$

491 Taking the supremum over all $x \in X$:

$$493 \quad \|Tv - Tu\| \leq \beta \|v - u\|, \quad (\text{A.3})$$

494 where $\|\cdot\|$ is the supremum norm. Thus by the definition, T is a contraction operator.

495 Rewrite Eq. (6) as

$$497 \quad v_n = Tv_{n-1} = T^n v_0$$

498 with arbitrary initial condition $v_0 \in V$, then by the Banach's fixed point theorem,

$$500 \quad \|v_n - v^*\| = \|T^n v_0 - v^*\| \leq \beta^n \|v_0 - v^*\|. \quad (\text{A.4})$$

501 Since $0 \leq \beta \leq 1$ and v is bounded,

$$503 \quad \lim_{n \rightarrow \infty} v_n \rightarrow v^* \quad (\text{A.5})$$

504 i.e., the optimal reward, or the solution of Eq. (4), exists and can be approximated by the value-iteration algo-
 505 rithm. The uniqueness of this solution is also guaranteed by the Banach's fixed point theorem.

506 References

- 507 Chang, G.L., Tao, X., 1997. Estimation of time-dependent turning fractions at signalized intersections. *Transportation Research Record*
 508 1644, 142–149.
- 509 Chang, G.-L., Wu, J., Lieu, H., 1994. Real-time incident-responsive corridor control: a successive linear programming approach. In:
 510 Proceedings of the Fourth Annual Meeting of IVHS America, Atlanta, GA, vol. 2, pp. 907–918.
- 511 Chen, A., Chootinan, P., Recker, W., 2005. Examining the quality of synthetic origin–destination trip table estimated by path flow
 512 estimator. *Journal of Transportation Engineering, American Society of Civil Engineers* 131 (7), 506–513.
- 513 Cremer, M., Schoof, S., 1989. On control strategies for urban traffic corridors. In: Proceedings of the XXX IFAC Conference on Control
 514 Computers and Communications in Transportation, Paris, France, pp. 213–219.
- 515 D'Ans, G.C., Gazis, D.C., 1976. Optimal control of oversaturated store-and forward transportation networks. *Transportation Science* 10,
 516 1–19.
- 517 Davis, G.A., Lan, C.J., 1995. Estimating intersection turning movement proportions from less-than-complete sets of traffic counts.
 518 *Transportation Research Record* 1510, 53–59.
- 519 Gartner, N., 1983. OPAC: A demand-responsive strategy for traffic signal control. *Transportation Research Record*, 906.
- 520 Hakimi, S.L., 1969. Analysis and design of communication networks with memory. *Journal of the Franklin Institute* 287 (1), 1–17.
- 521 Head, K.L., 1995. An event-based short-term traffic flow prediction model. *Transportation Research Record* 1510, 45–52.
- 522 Hernandez-Lerma, O., Lasserre, J.B., 1996. *Discrete-time Markov control processes Applications of Mathematics*, 30. Springer-Verlag.
- 523 Hunt, P.B., Robertson, D.I., et al., 1982. The SCOOT on-line traffic signal optimization technique. *Traffic Engineering and Control*.
 524 April.
- 525 Lin, F.B., 1989. Use of binary choice decision process for adaptive signal control. *Journal of Transportation Engineering*.
- 526 Lin, F.B., Vijayakumar, S., 1989. Adaptive signal control at isolated intersections. *Journal of Transportation Engineering*.
- 527 Lo, H.K., 2001. A cell-based traffic control formulation: strategies and benefits of dynamic timing plans. *Transportation Science* 35 (2),
 528 148–164.
- 529 Lowrie, P., 1982. The Sydney coordinated adaptive control system—principles, methodology, algorithms. In: IEE Conference Publication,
 530 207.
- 531 Mirchandani, P.B., Nobe, S., Wu, W., 2001. The use of on-line turning proportion estimation in real-time traffic-adaptive signal control.
 532 *Transportation Research Record* 1728, 80–86.

- 20 *X.-H. Yu, W.W. Recker / Transportation Research Part C xxx (2006) xxx–xxx*
- 533 Nakatsuji, T., Kaku, T., 1991. Development of a self-organizing traffic control system using neural network models. *Transportation*
534 *Research Record* 1324.
- 535 Papoulis, A., 1984. *Brownian Movement and Markoff Processes. Probability, Random Variables, and Stochastic Processes*, second ed.
536 McGraw-Hill, New York, pp. 515–553.
- 537 Robertson, D.I., 1969. TRANSYT: A traffic network study tool. RRL Report LR 253, Road Research Laboratory, England.
- 538 Robertson, D.I., Bretherton, R.D., 1991. Optimizing networks of traffic signals in real-time: the SCOOT method. *IEEE Transactions on*
539 *Vehicular Technology* 40, 1.
- 540 Singh, M.G., Tamura, H., 1974. Modelling and hierarchical optimization for oversaturated urban road traffic networks. *International*
541 *Journal of Control* 20 (6), 913–934.
- 542 Stephanedes, Y.J., Chang, K.-K., 1993. Optimal control of freeway corridors. *Journal of Transportation Engineering* 119 (4), 504–514.
- 543 Wilshire, R., Black, R., et al., 1985. *Traffic Control Systems Handbook*, FHWA-IP-85-12.
- 544 Yu, Nie, Zhang, H.M., Recker, W.W., 2005. Inferring origin–destination trip matrices with a decoupled GLS path flow estimator.
545 *Transportation Research Part B: Methodological* 39 (6), 497–518.
- 546

UNCORRECTED PROOF